A Generalization of the Forest Fire Model as an Epidemics Dynamics Model

Quan Manh Nguyen
Massachusetts Institute of Technology, 77 Massachusetts Ave., Cambridge, MA 02139
(Dated: May 20, 2023)

I review previous research on the forest fire model and a renormalization group treatment. I formulate an epidemic model as a generalization of the forest fire model, begin to construct a renormalization group (RG) treatment, and present some numerical simulation of the model.

I. INTRODUCTION

The forest-fire model was formulated in [1] and [2] on a grid in any dimensions. The dynamics includes a tree growth probability p from an empty site, an ignition probability f from a tree site, the spreading of fire from one site to its von Neumann nearest neighbors, and a burning site becoming an empty site in the next time step.

In the first few years, the model was touted as a prime example of a class of phenomena called *self-organized criticality* (SOC). An SOC does not have a precise definition, but roughly happens when the dynamics of the system drives the system towards the critical point, or the critical behavior exists independently of the initial conditions and over a wide range of parameter values, so no tuning of the parameters is needed [3, 4]. SOC was proposed to explain the apparent prevalence of critical phenomena in nature, including the magnitudes of earthquakes, forest fires, or neuronal avalanches. *Critical* here means that several observables have a power law distribution, without a length scale. In the paper that coined the term [5], the authors introduced the sandpile model, which, although does not describe real sandpiles [6], was proven to display criticality [7].

To facilitate analytical study of the forest fire model, in [8] and [9], Loreto and colleagues developed a block Renormalization Group (RG) scheme for the model in one and two dimensions in the double time scale separation $\theta = f/p \to 0$ and $p \to 0$.

However, in the following years, many results called into questions the validity of the preceding works. In [10, 11], intensive numerical simulation asserts that the forest fire model may not be critical after all. In other fields, the criticality of many SOC systems is still controversal [12–14].

Despite these doubts, the forest fire model is still an interesting model that can guide us towards an understanding of the spatial and temporal evolution of various phenomena in nature. In particular, it was soon realized (for example [15]) that the forest fire model provides a natural model for the spread of an epidemic. A tree corresponds to a susceptible individual, a burning site corresponds to an infected individual, and an empty site corresponds to a newly recovered individual with temporary immunity (in this paper we call it an immune individual). The ignition probability corresponds to the arrival of an infected individual to the community, or the transmission of the disease from animals to an individual. Here, the spread of the disease from an infected individual to a neighbor is not immediate, but with a probability q_1 each time step. A fire corresponds to an outbreak.

The organization of the paper is as follows. In section II, I introduce some important observables in the forest fire model and establish a connection between the forest fire model and epidemics dynamics. In section III, I review the real space renormalization group scheme for the forest fire model. In section IV, I present the first steps towards extending the scheme to the model of epidemics dynamics. I present some of my numerics for the epidemics dynamics model in section V. Finally, I discuss some future research direction in section VI.

II. FOREST FIRE AND EPIDEMICS DYNAMICS

A. Parameters and Observables of the Forest Fire Model

In the forest fire model as defined above, the dynamics do not depend on the absolute time scale $1/p$ or $1/f$, but depend on $\theta = f/p$. A cluster is defined as. The tree growth would increase the density of trees on the lattice, making it a site percolation system, until a fire burns down a cluster. Numerical simulations made in the 1990s is that the distribution of clusters with s sites is $P(s) \sim s^{-\tau}$ and average cluster radius scale is $R \sim \theta^{-\nu}$. The fractal dimension of clusters D is defined by $s \sim R^D$. The distribution of the time it takes to burn one cluster of size ξ is $T(\xi) \sim \xi^z$. Since $\xi \sim R$, $T(\xi) \sim \theta^{-\nu'}$ where $\nu' = \nu z$. In the limit $T(\xi) \ll 1/p$, there is no new tree popped up during the burning of a cluster, so we can think of each cluster burning as an individual event. Even though these scaling relations appear to break down when simulations explored smaller values of θ, a block renormalization group approach is still an interesting tool to explore this and related model, as well as to understand the limits of RG.

B. Connection to the Epidemics Model

In epidemics modeling, we mainly care about the number of infected individuals as a function of time, the number of immune individuals, the number of casualties, etc.

We also care about the distribution of outbreak size s: real life data was analyzed in [16], where it appears that the model in 3 or 5 dimensions would give a more accurate scaling exponent, even though definitive conclusions were lacking.

To better model the dynamics of an epidemic, I generalize the forest fire model by including a probability q_2 of disease spreading to a diagonal neighbor (a cell that share one vertex with the infected cell) and a probability r of an infected cell becoming an immune cell (the forest fire model fixes $r = 1$). I will construct an RG scheme with this generalization. In my simulations, I also include a probability s of death, after which the cell becomes inactive. From simulations, I extract the percentage of the population in each state, as well as a visualization of the spatial and temporal dynamics.

III. RENORMALIZATION GROUP FOR THE FOREST FIRE MODEL

In this section, we review the renormalization scheme for the forest fire model detailed in [9]. In the course-graining step, a cell at scale $(k + 1)$ is composed of b^d cells at scale k, where d is the dimension of the lattice. The parameters p and θ are renormalized to find the fixed point and the critical exponents near the fixed point. As we will see, the author made a number of approximations: they ignored the correlation in the occupation probability for nearby sites, and they determined that probability by the mean field densities of empty, green, and burning trees $\rho = (\rho_0, \rho_1, \rho_2)$ respectively. To calculate those, they assert that in the late time limit, the mean field densities at scale k are in the stationary state dictated by the master equations in d dimension with scale k parameters [17].

$$\rho_0' = (1 - p)\rho_0 + \rho_2 \tag{1}$$
$$\rho_1' = (1 - f - 2d\rho_2)\rho_1 + p\rho_0 \tag{2}$$
$$\rho_2' = (f + 2d\rho_2)\rho_1 \tag{3}$$

where ρ' is the density in the next time step, and is set equal to ρ to find the stationary state.

We will begin with RG in one dimension to build intuition, then proceed to RG in two dimensions which involves more approximations.

A. Forest Fire: RG in one dimension

Consider a scheme with $b = 2$. The authors defined the configurations at scale k that correspond to an empty site, a tree site, or a burning site at scale $(k + 1)$. A tree site at scale $(k + 1)$ is spanned by tree sites at scale k, while an empty site is not spanned. A burning site at scale $(k+1)$ is spanned by tree sites and has at least one burning site at scale k. These definitions ensure that the connectivity of tree sites and the spread of burning sites are preserved (see figure 1).

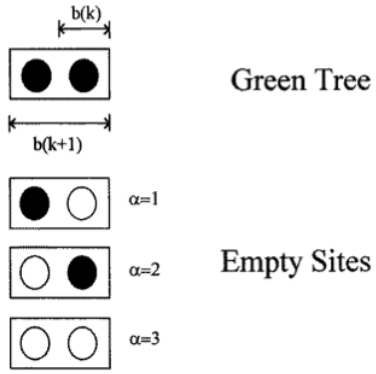

FIG. 1. Definition of states of a site in scale $(k + 1)$.

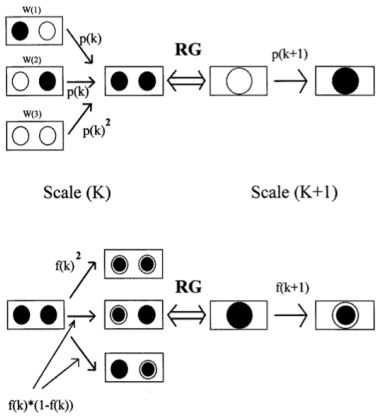

FIG. 2. Renormalization for p and θ in one dimension.

A parameter at scale $(k+1)$ is the probability of transition between configurations at scale $(k + 1)$, hence can be calculated from the total probability of transitions between the corresponding configurations at scale k (see figure 2).

$$p^{(k+1)} = W_1 p^{(k)} + W_2 p^{(k)} + W_3 \left(p^{(k)}\right)^2 \tag{4}$$
$$f^{(k+1)} = \left(f^{(k)}\right)^2 + 2f^{(k)}(1 - f^{(k)}) \tag{5}$$

where W_i is the probability of configuration i (in figure 2) at scale k given an empty site at scale $(k + 1)$. These renormalization equations assumed that fire spreading and tree growth are not interacting, corresponding to the time scale separation $p \ll \theta^{\nu'}$ mentioned before.

The weight W_i of each configuration is assigned by assuming neighboring sites have uncorrelated probabilities,

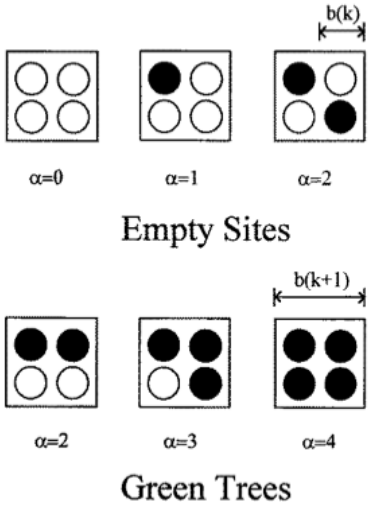

FIG. 3. Renormalization for p and θ in two dimensions.

which means

$$W_1 = W_2 = \frac{\rho_1^{(k)}}{\rho_0^{(k)} + 2\rho_1^{(k)}} \tag{6}$$

$$W_3 = \frac{\rho_0^{(k)}}{\rho_0^{(k)} + 2\rho_1^{(k)}} \tag{7}$$

For $d = 1$, the fixed point of the RG is $p^* = 0, \theta^* = 0, \rho^* = (0, 1, 0)$, with the linearized RG equations

$$\begin{pmatrix} p' \\ \theta' \end{pmatrix} = \begin{pmatrix} 1 & 0 \\ 0 & 2 \end{pmatrix} \begin{pmatrix} p \\ \theta \end{pmatrix} \tag{8}$$

There is one marginal and one relevant parameter. The relevant parameter θ has eigenvalue 2, thus a critical exponent $\nu = \frac{\log b}{\log \lambda_2} = 1.0$. Subsequent calculations show that $\tau = 1$ and $z = 1$, readers can refer to [9] for details. As mentioned before, with $\nu' = 1$ the above RG is only valid in the $p \ll \theta$ limit. In this limit, the critical exponents fit with the exact calculations in [18].

B. Forest Fire: RG in two dimensions

The structure of the renormalization procedure remains the same in two dimensions. The biggest difference lies in the definition of tree sites at scale $(k + 1)$. We want the definition to preserve the connectivity of tree clusters. For simplicity, the authors of [9] chose the left-right spanning condition, i.e. a tree site at scale $(k + 1)$ is spanned by tree sites at scale k in the horizontal direction. They claimed that different conditions, such as requiring spanning in both directions, converges to the same results with larger b (they only calculated $b = 2, 3$) and has the same general features of the flow diagram.

For $d = 2$, following detailed calculations in [9], we obtained the fixed point $p^* = 0, \theta^* = 0, \rho^* = (2/3, 1/3, 0)$, with the linearized RG equations

$$\begin{pmatrix} p' \\ \theta' \end{pmatrix} \approx \begin{pmatrix} 1.0 & 0 \\ 0 & 2.6 \end{pmatrix} \begin{pmatrix} p \\ \theta \end{pmatrix} \tag{9}$$

The critical exponents can be calculated as $\nu \approx 0.73$, $z \approx 1.11$, and $D \approx 1.7, \tau \approx 1.19$.

Many connected configurations were not accounted for properly by the $b = 2$ RG. Therefore, the authors performed a $b = 3$ RG with more complicated calculations and accounted for more connected configurations. They got $\nu \approx 0.65$ and $z \approx 1.02$. A calculation of the fractal dimension gives $D = 2$, leading to $\tau \approx 1.16$. These critical exponents improve on the $b = 2$ RG when compared to numerical results at the time, for example [19].

Notice that many of the issues with this approach in two dimensions is reminiscent of the usual Kadanoff's real space RG approach in equilibrium systems, such as the difficulty in accounting for all interactions.

IV. RENORMALIZATION GROUP FOR THE EPIDEMICS MODEL

In this section, we present the first calculations towards constructing an RG for the epidemics model with parameters (f, p, q_1, q_2, r) (we set the death rate $s = 0$ for simplicity). We work in the same limit as in the forest fire model: assume that an individual turning from immune to susceptible is rare compared to the spreading of an outbreak. We consider coarse-graining with $b = 2$. Note that any next-nearest neighbor spreading is renormalized to 0 when we do the coarse-graining, so we don't need to worry about those coefficients. We can also ignore q_2: in one dimension this term doesn't exist, while in two dimensions we will see that q_2 has an attractive fixed point at 0, in addition to our expectation that q_2 should be significantly smaller than q_1.

At scale $(k + 1)$, we define a susceptible individual as configurations with susceptible individuals spanning horizontally at scale k, and an infected individual as configurations with at least one infected individual at scale k. With these definitions, the renormalization equations for f and p are the same as in the forest fire model. Hence, we only need to consider the renormalization of r and q_1. These parameters characterize how different the dynamics is from the forest fire model: if $r \gg q_1$, infections cannot spread; if $r \lesssim q_1$, infections spreads effectively, similar to fires in the forest fire model. Smaller r only leads to longer lifetime of infections.

The master equations with these approximations in d dimensions are:

$$\rho_0' = (1 - p)\rho_0 + r\rho_2 \tag{10}$$

$$\rho_1' = (1 - f - 2dq_1\rho_2)\rho_1 + p\rho_0 \tag{11}$$

$$\rho_2' = (f + 2dq\rho_2)\rho_1 + (1 - r)\rho_2 \tag{12}$$

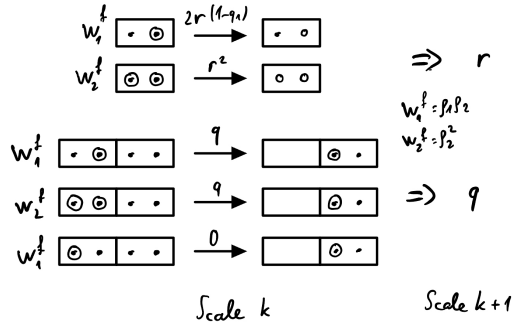

FIG. 4. Renormalization for r and $q \equiv q_1$ in one dimension.

In the following, we will only present the renormalization equations for q_2 and r in terms of the relative weights. We will not substitute the stationary equation in due to complicated algebra and lack of time. The calculations of the fixed point and critical exponents can be completed in a future work.

A. Epidemics: RG in one dimension

Because the infection does not spread automatically, whether an infection can spread at scale $(k+1)$ depends on if the scale-k configuration has an infection adjacent to the border. The renormalization is shown in figure 4.

B. Epidemics: RG in two dimensions

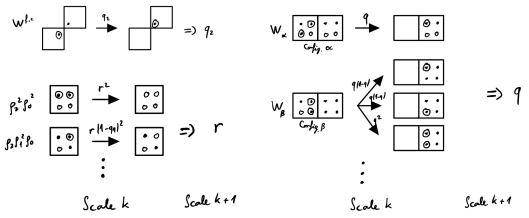

FIG. 5. Renormalization for q_2, r, and q_1 in two dimensions.

First we show that q_2 is irrelevant. The only configuration at scale k that corresponds to a q_2-spread at scale $(k+1)$ is in the upper left of figure 5. The relative weight $W^{f,c}$ conditioned on the site being a burning site is smaller than 1, hence the renormalization equation is $q_2^{(k+1)} = W^{f,c} q_2^{(k)}$ with eigenvalue smaller than 1. Because of this, we can take q_2 to be very small, ignoring its contribution to the renormalization fo q_1.

There are 12 configurations contributing to the renormalization of r and even more configurations for q_1. Here

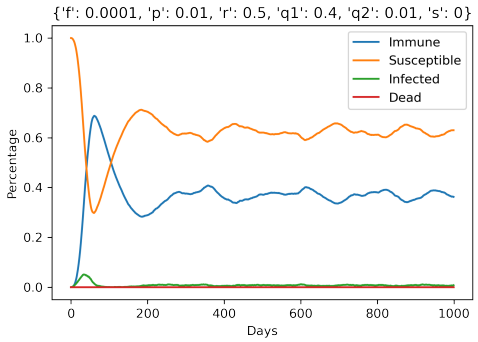

FIG. 6. Population breakdown as a function of time.

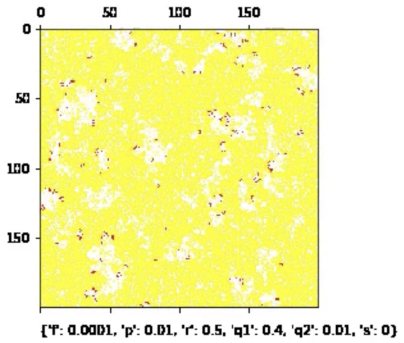

FIG. 7. A snapshot of the animation after the transient. Red cells are the infected, yellow cells are the susceptibles, and white cells are the immunes.

we only show two configurations for each, displayed in the lower left and the right of figure 5 respectively.

V. NUMERICAL

We present some numerical results of the epidemic model. We did not focus on cluster size, instead focused on population and visualization.

Below are figures from a run in a 200×200 lattice for 1000 time steps, with parameters shown in the first plot 6. We can see that after a transient, the populations of immunes and susceptibles are roughly stable at 0.37 and 0.62 respectively, while infection comes in regular small waves. In the snapshot 7, we can see fragmented infection fronts compared to the fire fronts in the forest fire model, as $q_1, q_2 < 1$ in this model.

For a bigger simulation in a 500×500 lattice with $\theta = p = 0.01$, $r = 0.2$, $q_1 = 0.4$, $q_2 = 0.2$, and $r = 0$, the infection front is less well-defined, as are the clusters.

VI. DISCUSSION

This project leaves open the calculation of RG for the epidemic model following the scheme presented here,

something that can be completed in future work. More insightful simulations should also be carried out to further understand this model and its validity when compared to real world epidemic data. The code and the algorithm for simulation can be optimized; currently running the aforementioned big simulation takes about an hour and saving the animation takes several hours.

An example for an area of improvement is to restructure the simulation to be able to extract the cluster size efficiently, so that we can find the critical exponents numerically.

Another interesting direction would be to model the effect of quarantines. A particular implementation could be as follows: every time an infected individual arrives (or an ignition occurs, in the forest fire language), the transmission coefficients q_1 and q_2 in an $m \times m$ area centered on the infected are decreased by a factor of, say, 2. The outbreak peaks and the number of deaths can be compared to the simulations without quarantines.

[1] P. Bak, K. Chen, and C. Tang, Physics Letters A **147**, 297 (1990), ISSN 0375-9601, URL https://www.sciencedirect.com/science/article/pii/037596019090451S.

[2] B. Drossel and F. Schwabl, Phys. Rev. Lett. **69**, 1629 (1992), URL https://link.aps.org/doi/10.1103/PhysRevLett.69.1629.

[3] D. L. Turcotte, Reports on Progress in Physics **62**, 1377 (1999), URL https://dx.doi.org/10.1088/0034-4885/62/10/201.

[4] R. Frigg, Studies in History and Philosophy of Science Part A **34**, 613 (2003), ISSN 0039-3681, URL https://www.sciencedirect.com/science/article/pii/S0039368103000463.

[5] P. Bak, C. Tang, and K. Wiesenfeld, Phys. Rev. Lett. **59**, 381 (1987), URL https://link.aps.org/doi/10.1103/PhysRevLett.59.381.

[6] V. Frette, K. Christensen, A. Malthe-Sørenssen, J. Feder, T. Jøssang, and P. Meakin, Nature (London) **379**, 49 (1996).

[7] D. Dhar, Phys. Rev. Lett. **64**, 1613 (1990), URL https://link.aps.org/doi/10.1103/PhysRevLett.64.1613.

[8] V. Loreto, L. Pietronero, A. Vespignani, and S. Zapperi, Phys. Rev. Lett. **75**, 465 (1995), URL https://link.aps.org/doi/10.1103/PhysRevLett.75.465.

[9] V. Loreto, A. Vespignani, and S. Zapperi, Journal of Physics A: Mathematical and General **29**, 2981 (1996), URL https://dx.doi.org/10.1088/0305-4470/29/12/008.

[10] P. Grassberger, New Journal of Physics **4**, 17 (2002), URL https://dx.doi.org/10.1088/1367-2630/4/1/317.

[11] G. Pruessner and H. J. Jensen, Physical Review E **65** (2002), URL https://doi.org/10.1103%2Fphysreve.65.056707.

[12] J. Beggs and N. Timme, Frontiers in Physiology **3** (2012), ISSN 1664-042X, URL https://www.frontiersin.org/articles/10.3389/fphys.2012.00163.

[13] J. O'Byrne and K. Jerbi, Trends in Neurosciences **45**, 820 (2022), ISSN 0166-2236, URL https://www.sciencedirect.com/science/article/pii/S0166223622001643.

[14] N. W. Watkins, G. Pruessner, S. C. Chapman, N. B. Crosby, and H. J. Jensen, Space Science Reviews **198**, 3 (2016).

[15] C. Rhodes and R. Anderson, Journal of the Franklin Institute **335**, 199 (1998), ISSN 0016-0032, part Special Issue on Biomathematics, URL https://www.sciencedirect.com/science/article/pii/S0016003296000968.

[16] C. J. Rhodes, H. J. Jensen, and R. M. Anderson, Proceedings of the Royal Society of London. Series B: Biological Sciences **264**, 1639 (1997).

[17] K. Christensen, H. Flyvbjerg, and Z. Olami, Physical review letters **71**, 2737 (1993).

[18] B. Drossel, S. Clar, and F. Schwabl, Physical review letters **71**, 3739 (1993).

[19] P. Grassberger, Journal of Physics A: Mathematical and General **26**, 2081 (1993).